Materials and Structures (2015) 48:2133–2146
DOI 10.1617/s11527-014-0298-3

ORIGINAL ARTICLE

Investigating the use of autoclaved aerated concrete as an infill in reinforced concrete sandwich panels

M. ElKashef · M. AbdelMooty

Received: 25 February 2013 / Accepted: 26 March 2014 / Published online: 1 April 2014

Abstract Reinforced concrete composite sandwich panels are typically made of two concrete wythes separated by an insulating core of rigid polystyrene foam. The strength of the panels relies mostly on the efficiency of the shear connectors between the two concrete wythes. The rigid foam is too weak in shear and provides no contribution to the shear resistance of the connectors. In this paper, autoclaved aerated concrete (AAC) is used as an insulating core in place of foam and its efficiency to transfer shear between the sandwich panel layers is investigated. A total of nine full scale specimens made of rigid foam and AAC are tested under flexural load with varying types of shear connectors. Their ultimate load capacities are compared and their respective modes of failure are discussed. A detailed analysis of the stiffness of the shear connectors is done and used to predict the deflection of the panels under the applied load.

M. ElKashef (✉)
Construction Engineering Department, The American University in Cairo, AUC Avenue, 5th Settlement, New Cairo, Egypt
e-mail: mkashif@aucegypt.edu

M. AbdelMooty
Structural Engineering Department, Faculty of Engineering, Cairo University, Giza, Egypt
e-mail: mamooty@aucegypt.edu

Keywords Sandwich panels · Autoclaved aerated concrete · Flexural capacity · Shear connectors

Abbrevations

List of symbols

A	Shear connector area
P	Total applied lateral load
b	Panel width
q_u	Maximum shear flow at support
c	Thickness of the inner core
Q	First moment of area of lower concrete wythe
d	Distance from center of upper wythe to center of lower wythe
Q_1	Shear force in panel associated with bending moment M_1
E_A	Modulus of elasticity of AAC
E_c	Modulus of elasticity of concrete
E_s	Shear connector modulus of elasticity
Q_2	Shear force in panel associated with the additional vertical deflection w_2
t	Thickness of the outer layer of the sandwich panel
F	Axial connector force
T_{max}	Maximum tension
G	Shear modulus of connector
I	Moment of inertia of the faces about the centroid of the sandwich
I_f	Sum of the moment of inertia of the faces about their own centroids

I_T Moment of inertia of the entire section
L Panel length
M_{max} Maximum moment
n Number of connector lines across panel width
p Shear connector slope
V_u Shear force at the support
w_1 Panel vertical deflection due to bending deformation of the panel
w_2 Panel vertical deflection due to shear stress in the core
γ Inner core shear deformation
τ Shear stress in the core
τ_{ave} Average shear stress
τ_{max} Maximum shear stress

1 Introduction

The use of composite sandwich panels has recently grown in popularity due to the emerging trend to shift to energy efficient structures. They have a wide range of versatile applications in the aerospace, marine, transportation and construction industries. Reinforced concrete sandwich panels are composite structures made of two outer layers of concrete with a light-weight thermally insulating core in between. Wall sandwich panels were first introduced in 1960s with a design utilizing double tees. Other designs including hollow cores and flat slabs were later introduced. The insulating core is usually made of honeycomb or rigid polystyrene foam with high thermal insulating properties. The panels can be designed to withstand both in-plane and out-of-plane forces. According to load demands, they can be prestressed or non-prestressed. The panels act much like an I-beam where the concrete skin behaves as flanges to resist bending stresses and the inner core correlates with the web of the I-beam in resisting shear only.

The structural efficiency of the panel relies mostly on the degree of composite action between the outer and inner concrete wythes. Several shear transfer mechanisms are available including the friction between the concrete and the insulating core, use of concrete web connectors and use of metallic or non-metallic shear connectors. Shear connectors are available in a variety of configurations including trusses, pins, rods and grids. The type, spacing and arrangement of the shear connectors allow the panel to act as partially to fully composite. A full composite action is achieved when the panel behaves as one unit in a way similar to a solid slab. In partially composite panels, local bending would occur in each of the concrete wythes. The several aspects pertaining to the use, design, manufacturing and detailing of sandwich panels have been covered in depth in the report prepared by the PCI committee on precast sandwich wall panels [1].

Sandwich panels have been under extensive research in the recent decades. The work done in [2] comprised testing of more than 50 non-prestressed sandwich panels under flexure. The panels used different types of shear connectors. Both the type and spacing of the shear connectors were shown to have a great impact on the degree of composite action of the panels. The use of truss shaped metal connectors was most efficient. Other types of metal connectors with no diagonal members did not prove as efficient. More panels were tested in [3] using truss shaped connectors. These tests investigated the effect of varying the number, orientation and spacing of the connectors. It was shown that the best orientation is achieved when the connectors are laid longitudinally along the entire length of the panels. It was also shown that the friction between the layers of the sandwich panels did not contribute significantly to the shear transfer. The effect of using solid concrete regions as shear transfer mechanism was investigated in [4] where four full-scale precast concrete sandwich panels were tested under uniform lateral load. It was shown that with proper design, the solid concrete regions could be arranged to achieve a full composite action. Solid concrete regions however drastically reduce the thermal efficiency of the panels. To increase the thermal efficiency of the panels, a new system of fiber reinforced plastic connectors was developed in [5]. The test results showed that these types of connectors achieved a high level of composite action in addition to a significant improvement in the thermal efficiency over metal type connectors. An experimental study [6] was conducted to evaluate the performance of a variety of domestically available shear connectors including steel clips, welded wire steel truss, carbon fiber reinforced plastic grids, and glass fiber reinforced plastic pins. The results showed that the connectors have a considerable variation in strength, stiffness and deformability.

In this study, autoclaved aerated concrete (AAC) is introduced as a viable alternative to rigid foam. AAC

has a relatively higher shear modulus compared to rigid foam and could possibly contribute to the shear transfer between the concrete wythes. AAC is also considered green since it is manufactured using abundant and natural raw materials as it is made of silica, cement, lime, water, and an expansion agent—aluminum powder. AAC is 80 % voids and has a thermal conductivity of as low as 7 % of normal concrete.

2 Overview of composite sandwich panel theories

An extensive work has been done over the years to develop analytical theories in order to model the behavior of sandwich panels. The so-called classical sandwich panel theories, originated by [7], gave a mathematical description of the deformation of the panels. In the work done by Allen, the total displacement of the panel is divided into two parts, as shown in Fig. 1. In the primary deformation, the panel undergoes a vertical deflection due to pure bending without taking into account the effect of the shear deformation. The effect of the shear deformation of the weak core would cause the panel to undergo an additional vertical deflection and the outer layers of the sandwich panel to bend about their own neutral axes. This theory is based on a main assumption of an "antiplane" core where the core is treated as an idealized material which has a zero modulus of elasticity in a direction parallel to the faces and an infinite modulus of elasticity in the direction perpendicular to the faces. This means that the core makes no contribution to the bending stiffness of the panel and it also means that the deflections of the upper and lower faces are equal to each other. It also follows that a constant shear stress exists over the core depth. The classical theory was further developed by a number of researchers [8, 9] to introduce the superposition approach which deals with local effects including wrinkling of faces and localized loads. In this approach, the local effects are formulated separately and superposed on a general solution of the whole panel using the classical theory. Later on, higher order theories [10] were developed to account for panels with non-antiplane cores where the core is flexible in the transverse direction and the boundary conditions are not the same throughout the entire height of the panel section. With the use of higher order theories, it was possible to analyze panels with point loads and point support regions, edge and inner delamination regions, overall buckling behavior, edge and inner transverse diaphragms, cut-off edge connection and unsymmetric laminated composite faces. A study conducted by [11] presented an overview of the sandwich panel theories and a comparison was made between the different theories. It was shown that the overall behavior of sandwich panels can be predicted with fair accuracy using the classical theory. The use of higher order theories should be used when the study of local effects is important since it takes into account all influences through the thickness of the sandwich panel. The study of reinforced concrete sandwich panels do not call for the use of higher order theories since these types of panels will not experience failures of the type described above. In this paper, Allen's classical theory is used to analyze the experimental results. A brief overview of Allen's theory is given in the appendix where the governing differential equation relating loads and deformation is derived. The governing differential equation is solved for a panel subjected to a 4-point loading and an expression for the vertical deflection of the panel is obtained.

3 Experimental programme

3.1 Test specimens

The experimental programme was designed to investigate the performance of RC sandwich panels under a number of parameters which include the effect of using AAC infill in place of rigid foam as an inner core, also the use of different types and sizes of shear connectors. A total of twelve full scale specimens measuring 1 m wide and 3 m long and spanned 2.8 m between lines of support were tested under a 4-point lateral loading test. All panels had a total thickness of 200 mm and were made of two 50 mm thick concrete wythes separated by a 100 mm insulating core. Four panels were constructed using foam, out of which two specimens used truss shaped connectors of size 8 mm, denoted hereinafter as FS8-1 and FS8-2, the other two specimens used concrete web connectors reinforced with stirrups of size 8 mm, denoted hereinafter as FW8-1 and FW8-2. Two panels used AAC, one using 8 mm truss shaped connectors to be referred to as AS8, and the other one using concrete web connectors with 8 mm stirrups, denoted as AW8. To study the effect of

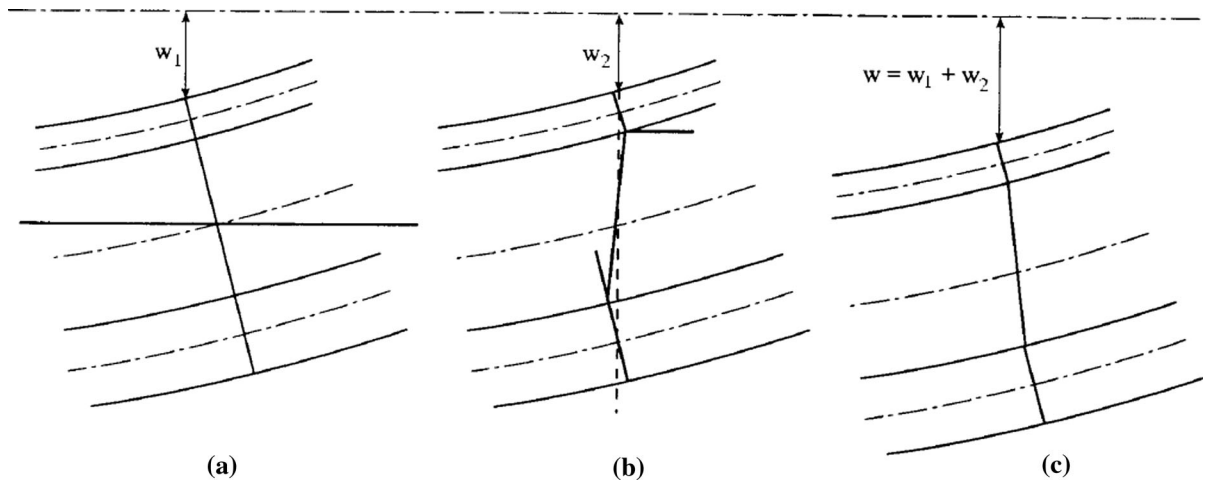

Fig. 1 Deflection according to classical theories. **a** Deflection due to pure bending. **b** Deflection due to shear deformation, and **c** Total deflection

Table 1 List of Tested Specimens

Specimen	Type of connector	Size of stirrups/ truss-shaped connector (mm)	Inner core
FS8-1	Truss-shaped steel	8	Foam
FW8-1/2	Concrete web	8	Foam
AS8	Truss-shaped steel	8	AAC
AW8	Concrete web	8	AAC
AS6-1	Truss-shaped steel	6	AAC
AW6-1	Concrete web	6	AAC
AN-1/2	None	–	AAC

varying the size of the shear connectors, two panels were tested using AAC and truss shaped steel connectors of size 6 mm, AS6-1 and AS6-2, also two panels were tested using AAC but with concrete web connectors with 6 mm stirrups, AW6-1 and AW6-2. Two more panels were tested where no shear connectors of any type were used and the surface of the AAC blocks was roughened to increase the friction between AAC and the concrete layers, AN-1 and AN-2. Three out of the twelve specimens have shown erroneous results during testing due to flaws in their construction. These specimens, namely, FS8-2, AS6-2 and AW6-2 will be discarded. A summary of the remaining nine specimens is listed in Table 1.

The reinforcement layout of all specimens is shown in Fig. 2. The reinforcement used in the concrete wythes was identical for all specimens. For the bottom wythe, six 12-mm bars were used in the longitudinal direction and sixteen 8-mm bars in the transverse direction. The top wythe had six 10-mm bars in the longitudinal direction and sixteen 8-mm bars in the transverse direction. The reinforcement in the top wythe was provided to control cracks due to shrinkage and to resist local bending which could possibly occur due to lack of full composite behavior. Two lines of truss shaped connectors laid longitudinally and continuously along the entire length of the panel were used for all panels utilizing steel connectors. The slope of the truss diagonals was nearly equal to 1. The transverse reinforcements were allowed to cross over the truss connectors to ensure proper interlinking with the concrete wythes. As for the panels with web connectors, two 50-mm wide concrete webs were used to interconnect the two concrete wythes. These webs were reinforced with stirrups placed at 100 mm spacing along the entire length of the panel. The yield stress of the used reinforcement bars was 400 MPa while the yield stress of the stirrups and steel shear connectors was 250 MPa. The average 28-day cube compressive strength for concrete was 45 MPa. The tensile splitting strength for concrete was also determined according to ASTM C496 to be 3.1 MPa. The compressive strength of the AAC blocks used was 2.98 MPa and its tensile strength 0.3 MPa. The elastic moduli of the concrete and AAC were determined to be 23,500 and 2,180 MPa respectively.

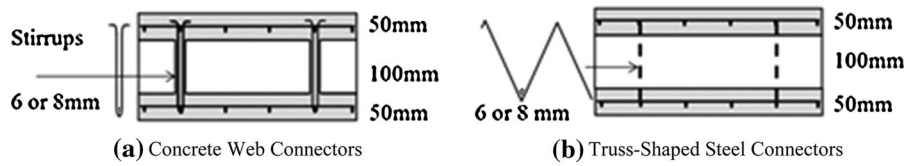

Fig. 2 Reinforcement layout for the different types of specimens

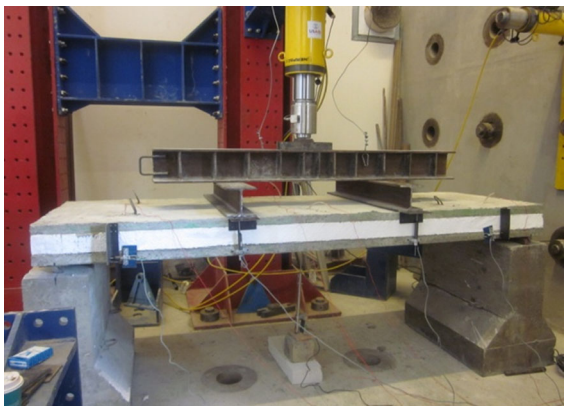

Fig. 3 Test set-up for 4-point loading

The specimens were prepared in the lab in a horizontal position by pouring the bottom wythe first followed by placing the insulating core on top of the fresh concrete and then pouring the top wythe. While placing the AAC blocks, they were soaked in water prior to their placement to avoid absorption of water from concrete. A retarder was used for the concrete to delay its initial setting time and allow the AAC to bond properly to the fresh concrete. The AAC blocks were readily available in the construction market in standard sizes of 600 × 200 mm and thickness of 100 mm. A full size AAC panel of dimension 1,000 × 3,000 mm could equally have been used to avoid having joints between the AAC blocks however these were not available in the market.

3.2 Test set-up and instrumentation

The load was applied through a hydraulic jack using a hydraulic pump with a pressure regulator to set the loading to an appropriate rate to allow careful observation of the behavior of the panels during testing. The load was transferred to the panel using a large steel I-beam and two smaller I-beams placed at mid-thirds of the panel to create two line loads as shown in Fig. 3. A simply supported end condition was simulated using steel line rollers to allow for horizontal movement due to bending and to minimize local stresses at the supports.

The behavior of the panels during testing was monitored and recorded through careful placement of surface mounted strain gauges and LVDTs. The total applied load is measured using a 200 ton capacity load cell connected to the hydraulic actuator of the same capacity. To measure the vertical deflection of the panels, an LVDT was placed at the mid-span point of the lower concrete wythe. The degree of composite action between the two concrete wythes was determined through measuring of the relative horizontal and vertical deformation between the two wythes. The differential vertical deflection was measured at the two points of load application as depicted in Fig. 4. As for the differential horizontal sliding, a steel angle was fixed to the upper concrete wythe and an LVDT was mounted horizontally on the lower wythe and made in contact with the angle. The movement of the steel angle was detected by the LVDT indicating the differential movement between the two concrete wythes. The strains in the top and bottom longitudinal reinforcement are also measured at mid-span using four surface mounted electrical strain gauges two in each wythe. Electrical strain gauges are also attached to the steel shear connectors and to the steel stirrups.

4 Test results

4.1 Load deflection curves

The total applied lateral load was plotted against the vertical deflection at midspan. Figure 5 shows the load deflection curves for the panels using 8-mm size connectors and stirrups. All panels with concrete web connectors whether made of AAC or foam showed a considerably higher ultimate load capacity. There was no noticeable difference in the behavior of the panels made of AAC or foam when concrete web connectors are used. Hence, AAC provided no improvement for such types of panels. The failure of these panels was

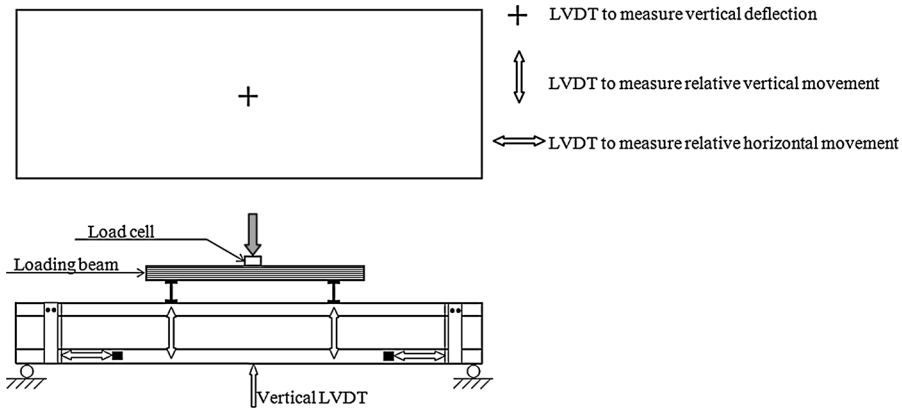

Fig. 4 Instrumentation layout

due to yielding of the main reinforcement in the concrete wythes, so it can be fairly said that the concrete web connectors, acting alone, provided sufficient shear resistance until failure and the inner core did not contribute to the shear resistance, hence the material of the inner core being AAC or foam did not affect the ultimate strength. The inner core whether being AAC or foam did not add to the strength of the panels. In the case of panels with truss-shaped steel connectors, failure was at a much lower load due to failure of the shear connectors. For these panels, although the ultimate load was the same for both AAC and foam but the behavior of the panels with AAC was better in terms of stiffness and ductility. Panels with AAC and 8-mm size truss shaped connectors exhibited a fully composite behavior until just prior to failure. The failure of these panels showed a more ductile behavior compared to panels with foam which failed suddenly upon failure of the connectors. The use of AAC helped to sustain the load capacity of the panel beyond the failure of the steel connectors. The higher stiffness and better ductility behavior is an advantage brought by the use of AAC when 8-mm size shear connectors were used.

The load-deflection curves of the panels using 6-mm connectors and stirrups are shown in Fig. 6. Only panels with AAC were tested in this phase of the test programme. AAC panels with no web connectors were also included for comparison. Again, it can be shown that panels with web connectors had a higher ultimate load capacity. However, the difference between the panels with web connectors and those with shear connectors were not that drastic as was the case when 8-mm size connectors. Through a careful study of Fig. 6, it can be argued that the use of AAC may have

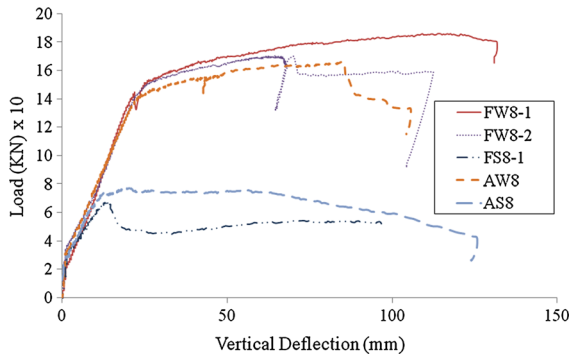

Fig. 5 Load-deflection curves for specimens with 8-mm size connectors and stirrups

slightly increased the ultimate capacity of the panels. For panel AS6-1, the shear connectors started to fail at a load of about 50 KN, marked by the sudden drop of load at this point in the curve; however a further increase in the load capacity was observed beyond this point. This further increase is possibly attributed to AAC being able to redistribute the load along the panel. It can be observed that the ultimate load resisted by AS6-1 using 6-mm connectors was almost equal to the panel AS8 using 8-mm connectors. It could be argued that the diameter of the truss shaped connectors was not the limiting factor in the failure of the two panels. It is clear that the 6-mm truss shaped connectors did not withstand a high load and it failed at an early stage however the panel continued to carry more load possibly due to the presence of AAC which managed to retain the integrity of the panel. However, this noted increase in load when using AAC can not be ascertained based only on the current series of tests and further testing is required to verify this, since this increase was only true for panels with 6-mm size connectors whereas no such increase

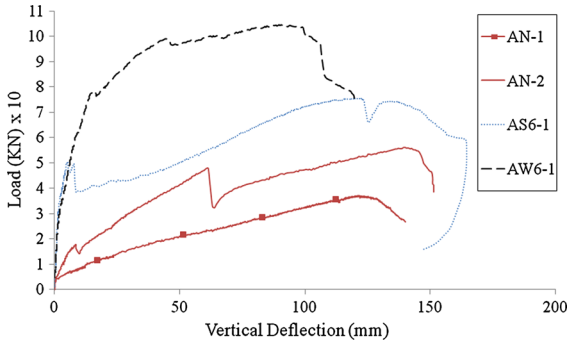

Fig. 6 Load-deflection curve for specimens with 6-mm size connectors and stirrups

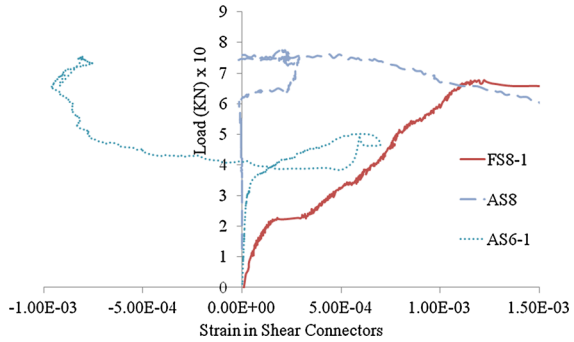

Fig. 7 Strains in shear connectors for panels using truss-shaped connectors

occurred for panels with 8-mm size connectors. Additionally no panels with foam using 6-mm size connectors were tested and hence no comparison is available between AAC and foam for such type of connectors. From the load deflection curves in both Figs. 5 and 6, it can also be seen that all panels exhibited the same initial stiffness before they started to lose stiffness. A detailed analysis of the stiffness will follow in Sect. 5.

4.2 Strains in shear connectors

Figure 7 shows the strains in the connectors for all specimens using truss-shaped steel connectors. The difference between the panels with AAC and those with foam is very obvious. The strain in the connectors for the panels with AAC was very low until just prior to failure. This indicates that AAC contributed to the shear resistance and carried part of the shear stress along with the connectors. The negative strain readings in the shear connectors of AS6-1 are not indicative since they were recorded following yielding of the steel connectors. Specimen AS6-1 is of particular interest though because it continued to carry load further to yielding of the steel connectors as discussed in Sect. 4.1.

4.3 Relative horizontal sliding

The relative horizontal sliding for panels using 8-mm size connectors, shown in Fig. 8, is an indication of the degree of composite action in the sandwich panels. A very small relative horizontal sliding marks a high degree of composite action which was true for panels with AAC. Panels using foam showed a comparatively higher relative horizontal sliding indicating a loss of full composite action at earlier stages of loading. It is

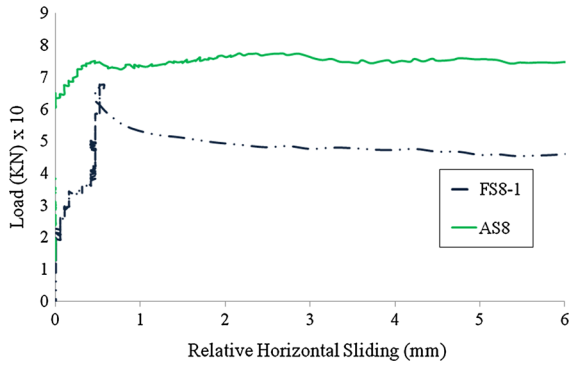

Fig. 8 Relative horizontal sliding in panels using 8-mm truss-shaped connectors

seen in Fig. 8 that panel AS8 continued to show a full composite action until just prior to failure. This was not the case for panels FS8-1 which exhibited a partial composite action at values of loading far less than the ultimate load. The failure of these panels is marked by an increase in the relative horizontal sliding with no increase in load which indicates a state of non-composite action of the panels where each of the two concrete wythe starts to act independently.

4.4 Failure mechanism

A study of the strains in the longitudinal reinforcement shown in Fig. 9 would give us a clue about the type of failure of the panel. It can be shown that failure of the panels with web connectors occurred as a result of yielding of the main reinforcement. However in the case of panels with steel connectors, a premature failure occurred way before yielding of the main reinforcement due to failure of the shear connection

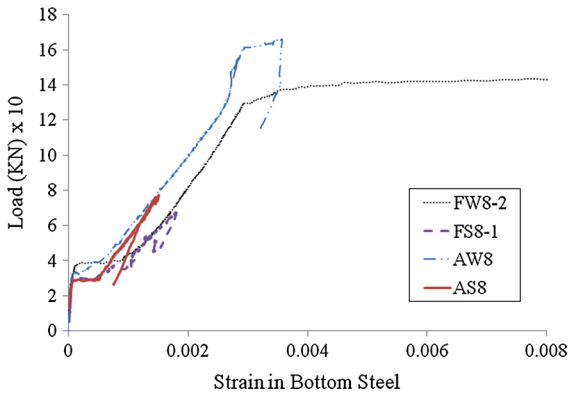

Fig. 9 Strain in longitudinal steel in the bottom wythe

mechanism. For such panels, it is clear that the strains in the bottom steel for the panels did not reach yielding strain at the time the panels failed. This was true for both panels using AAC and foam. Note that the horizontal plateau at a load of 30–40 KN indicates the initiation of concrete tensile cracks in the lower concrete wythe.

5 Analysis of shear connectors' stiffness

The stiffness of the shear connectors is directly related to the relative horizontal slippage between the two concrete wythes. As a result of the applied load, the sandwich panels will undergo bending deformation which will induce a shear stress between the different layers of the sandwich panel. The role of the shear connectors is to resist this shear stress and hold together the different layers of the panel. The value of this shear stress can be calculated from the lateral applied load. The effectiveness of the shear connectors in making the panel behave as one unit is determined by its stiffness. It is thus very crucial to evaluate this stiffness. The calculated shear stress along with the value of the measured relative horizontal slippage can be used to determine an experimental value for the stiffness. An estimate of the connector's stiffness can also be obtained analytically and compared to the experimental value.

5.1 Analytical value for the stiffness

In order to analyze the stiffness of the truss-shaped connectors, one need to calculate the forces and

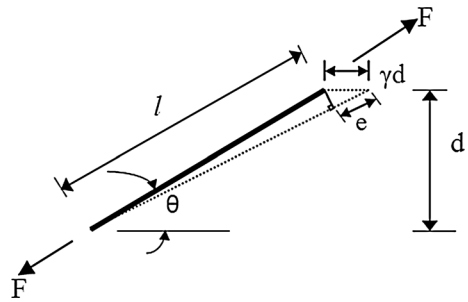

Fig. 10 Axial elongation of steel shear connectors

deformations developed in the truss members. In doing so, the truss members are assumed to be pinned at the center of each wythe. This assumption is valid since earlier research [12] has shown that for a truss diagonal at this inclination, the bending stiffness is less than 1 percent of the axial stiffness.

Using the illustration in Fig. 10, a shear deformation γ of the core, would cause an elongation e in the connector,

$$\mathrm{e} = \gamma \mathrm{d} \cos(\theta) \tag{1}$$

The axial connector force F is given, as follows:

$$F = (\mathrm{e}/l)E_s A = \gamma \cos(\theta) \sin(\theta) E_s A = \gamma \cos^2(\theta) p E_s A \tag{2}$$

Noting that $\cos^2(\theta) = 1/(1+p^2)$,where p is the slope of the shear connector, and considering a unit shear deformation γ; Equation 2 can be re-written as:

$$F = pE_s A/\left(1+p^2\right) \tag{3}$$

where A is the connector's area and E_s is the connector's modulus of elasticity.

The shear modulus of the connector, G, is the component of F parallel to the wythe divided by its tributary area. The tributary area is defined as db/np, where n is the number of connector lines across the panel width, b and d is the distance from center of upper wythe to center of lower wythe.

$$G = E_s A n p^2/db\left(1+p^2\right)^{3/2} \tag{4}$$

Substituting for $p = 1$, $d = 150$ mm, $b = 1{,}000$ mm, $E_s = 200\text{e}3$ MPa, $n = 2$ and using 8 mm size connector, one can get the effective shear modulus for the truss-shaped steel connector $G = 48$ MPa. For 6 mm size connector, the shear modulus would be $G = 27$ MPa.

5.2 Experimental value for the stiffness

The shear stress sustained by the panels is calculated here below using two different approaches. The first approach entails using the PCI [1] recommendation whereas the second approach is based on the calculation of the maximum shear flow at the support interface. The shear stress is calculated using the two approaches and the difference in calculation was insignificant.

Since steel yielding of the shear connectors will allow redistribution of shear flow over the entire length of the panel, the design of the connectors can be based on an average shear flow rather than the maximum shear flow near the support. For uniform loading, PCI [1] recommends calculation of the tension/compression force at midspan and dividing it by the shear span, which is half the length of the panel, to get an average shear flow to be used in the design of shear connectors. In the case of 4-point loading, the shear span is one third of the panel length.

The maximum moment in the panel can be expressed as $M_{max} = PL/6$, the maximum tension, T_{max}, can then be computed as $T_{max} = M_{max}/d$. The average stress is thus given by,

$$\begin{aligned} \tau_{ave} &= T_{max}/(bL/3) \\ \tau_{ave} &= 0.00326\ P(\text{MPa}) \end{aligned} \tag{5}$$

where P is the total applied lateral load in KN.

Alternatively, we can calculate the maximum shear flow at the interface between concrete and AAC, at the support using:

$$q_u = V_u \sum QE \Big/ EI_T \tag{6}$$

where q_u is the maximum shear flow, V_u is the shear force at the support, Q is the first moment of area, E modulus of elasticity and I_T moment of inertia of the entire section.

$\sum QE$ is calculated for the area below the interface line, i.e. lower concrete wythe.

$$\sum QE = E_c btd/2 = 8.81\text{e}10\ \text{Nmm}$$

where E_c is the modulus of elasticity of concrete and t is the thickness of the concrete wythe.

$$\begin{aligned} EI_T &= E_c bt^3/6 + E_c btd^2/2 + E_A bc^3/12 \\ &= 1.38\text{e}13\ \text{Nmm}^2 \end{aligned}$$

where E_A is the modulus of elasticity of AAC and c is the thickness of the inner core.where, $b = 1{,}000$ mm, $t = 50$ mm, $c = 100$ mm, $d = 150$ mm, $E_c = 23{,}500$ MPa, $E_A = 2{,}180$ MPa.

$$\begin{aligned} V_u &= P/2 \\ \tau_{max} &= q_u/b = 0.00313\,P\,(\text{MPa}) \end{aligned} \tag{7}$$

The shear stress calculated through both Eqs. 5 and Eq. 7 is almost equal, so either one of the two approaches could be used to determine the shear stress. It should be noted that both Eqs. 5 and 7 are based on the assumption that the concrete is in its un-cracked stage.

The maximum shear stress, as calculated from Eq. 7, was plotted against the shear strain in Fig. 11a. The shear strain was obtained by dividing the relative horizontal sliding over the distance d. Figure 11a was used to construct a multi-linear curve, Fig. 11b, using the least-square method for curve fitting, to idealize the response of each type of panel. The multi-linear backbone curve generally constitutes three regions; fully composite, partially composite and plastic yielding. Figure 11b shows the backbone curves developed for the panels using steel connectors. This figure can be used to derive information about the stiffness of the shear connectors. Better performance was noted in case of the panel AS8, with AAC, compared to the slab FS8, with foam. The use of AAC allowed the panel to act as one unit until just prior to failure. The panel FS8 started to behave as partially composite at a shear stress of about 0.08 MPa with a stiffness of 33 MPa as determined from the backbone curve. The panel AS6, using truss shaped connectors, also showed a fully composite behavior at the onset of loading until a load of 0.06 MPa where it started to exhibit a partially composite behavior. The measured stiffness using the backbone curve was different from the analytical stiffness of 48 MPa calculated using Eq. 4.

The reason for this difference may be attributed to sliding of the connectors from their original position against the concrete wythe. The amount of this sliding is related to a number of factors including the connectors embedment length into the concrete wythe in addition to the interlink between the connectors and the main reinforcement.

Similar curves were also obtained for the panels with web connectors as shown in Fig. 12. The panels,

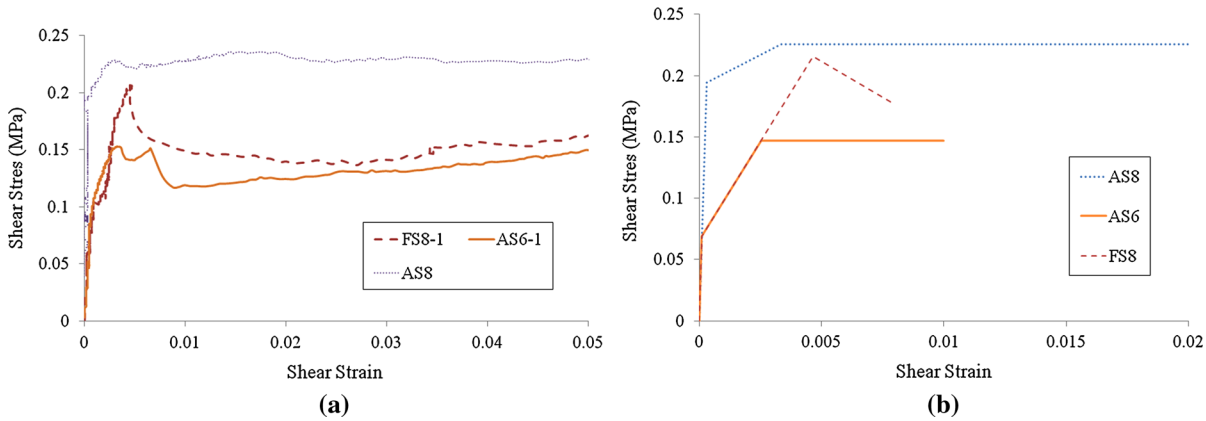

Fig. 11 Shear stress vs shear Strain for the panels with shear connectors (**a**) and multi-linear backbone curve (**b**)

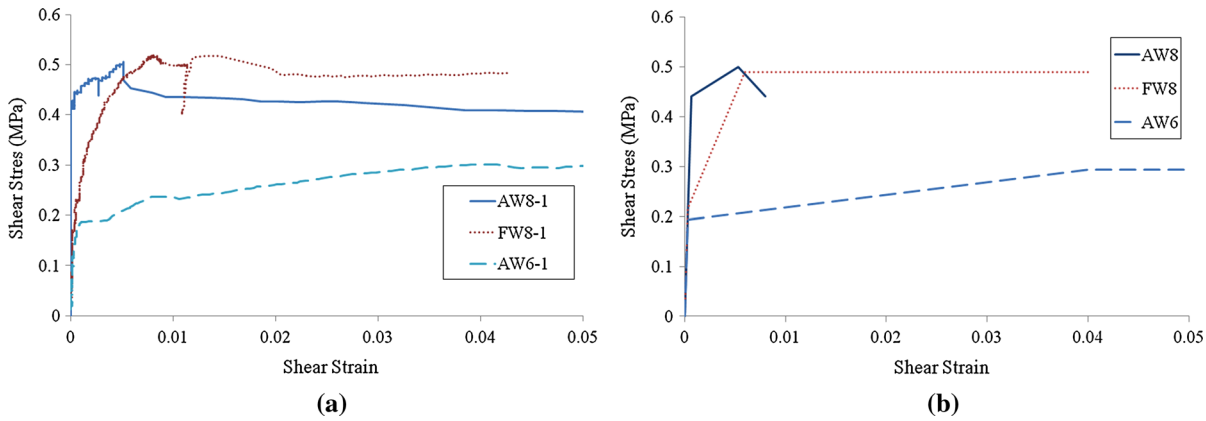

Fig. 12 Shear stress vs shear Strain for the panels with web connectors (**a**) and multi-linear backbone curve (**b**)

AW8, with AAC, maintained a fully composite behavior until failure. Whereas, the panels with foam, FW8, started to behave in a partially composite manner at a shear stress of about 0.2 MPa with a measured stiffness of 50 MPa. With regards to the panels, AW6, a fully composite behavior was noted until a shear stress of about 0.2 MPa, followed by a reduction in stiffness possibly due to yielding of the stirrups. The stiffness measured beyond this yielding point matches the stiffness of the panel with no connectors.

AAC shows to be successful in retaining the integrity of the panel to act as one unit regardless of the type of connector used. At the onset of loading, both types of panels are acting as fully composite. At higher loads, when specimens start to show tensile cracks and friction between the concrete and the inner core is reduced, AAC continues to resist shear stress along with the connectors thus maintaining the fully composite action.

6 Comparison of experimental and theoretical load deflection behavior

The vertical maximum deflection at midspan is a function of both shear deformation as well as bending deformation. In the case of sandwich panels, the shear deformation is significant and thus cannot be neglected. The shear deformation is determined largely by the shear modulus of the inner core. A general differential equation was derived by [7], $Q_1'' - a^2 Q_1 = -a^2 Q$, where the term $a^2 = AG/EI_f(1 - I_f/I)$ is a measure of the inner core shear modulus relative to the panel flexural stiffness. This equation was used to derive an expression for the

maximum deflection at mid-span for the particular case of 4-point loading, Eqs. 14 and 15, in the appendix. Equations 14 and 15 take into account the vertical deflection due to both bending and shear deformation. In the case of a fully composite panel, where the shear modulus is very high, the effect of the shear deformation is negligible. As the shear modulus decreases, the contribution of the shear deformation to the overall deformation becomes significant. The value of the experimental shear modulus for the connector obtained in the previous section can be used as input to the derived equations, Eqs. 14 and 15, in order to draw a theoretical plot for the load deflection curve. The experimental value for the shear modulus is used in lieu of the analytical value since it provides a more realistic value which takes into account the interconnection between the connectors and the concrete wythe as outlined in Sect. 5.2 above.

For the panels with web connectors, a high stiffness was used to model a fully composite action. This stiffness was assumed constant while plotting the whole curve since no decrease in stiffness was shown when using AAC. There was a slight decrease in stiffness in the case of foam but this was inconsiderable and thus ignored. The calculated curve took into account the decreasing value of the moment of inertia of the section due to tensile cracks in the bottom wythes. The curve obtained was in close agreement to the experimental curves as shown in Fig. 13.

For the panels with truss shaped connectors, an initial high stiffness was used as obtained from the backbone curve. This stiffness was decreased following a load of 20 KN as determined from the backbone curve. Figure 14 shows that the developed curve is very close to the experimental curve. The experimentally measured deflection is on the higher side which seems reasonable since the moment of inertia used in the calculation does not take into account the further reduction caused by tensile cracks in the upper wythe due to local bending.

7 Summary and conclusion

The flexural behavior of composite sandwich panels with both foam and AAC inner core was investigated where a total of nine full scale panels measuring 1,000 × 3,000 mm were tested under 4-point lateral loading. The tested panels used different shear connectors including truss-shaped steel connectors and concrete web connectors. Panels with no shear connectors were also tested for comparison. It was shown that using two lines of 50-mm wide web connectors reinforced with 8-mm stirrups placed every 100 mm was capable of resisting the shear between the two concrete wythes until failure occurred due to yielding of the main reinforcement of the bottom wythe. All other tested panels failed earlier due to the failure of the shear connectors. It was shown that the use of AAC as an inner core enhanced the performance of the panels with regards to stiffness and mode of failure. Panels which used AAC exhibited a full composite behavior until failure. A ductile mode of failure was also observed when AAC was used. However, no increase in the ultimate capacity was

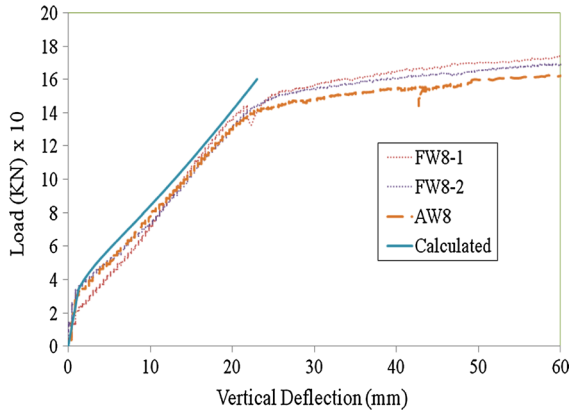

Fig. 13 Panels with concrete web connectors using 8-mm stirrups

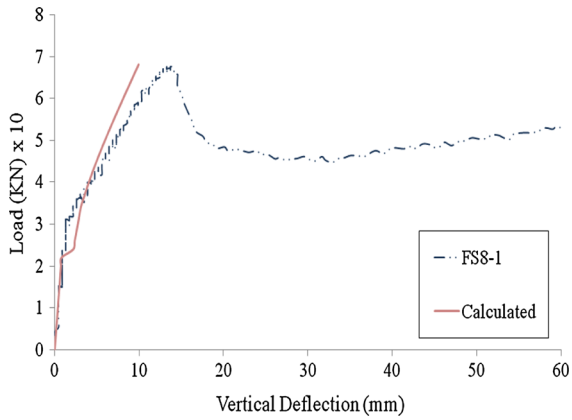

Fig. 14 Panels with truss-shaped steel connectors of size 8-mm

noted when AAC was used, except for the panels using 6 mm truss-shaped connectors which showed a slight increase in ultimate capacity. Nonetheless, further testing need to be done to verify this increase in ultimate capacity. The benefit of using AAC was clearly evident for panels with truss shaped connectors. Upon failure of the truss connectors, AAC was capable of sustaining the same load at an increasing deflection prior to failure unlike panels with foam which showed a sudden type of failure. In the case of panels with web connectors, the difference between AAC and foam was insignificant.

A close correlation between the stiffness of the shear connectors and the overall panel vertical deflection is noted. All panels exhibited an initial fully composite behavior before the stiffness starts to decrease. The relative horizontal sliding between the two concrete wythes was used to calculate an experimental value for the stiffness of the shear connectors. This experimental value for the stiffness compared well to the analytical value. A multi-linear curve was constructed for each type of panel to represent the stiffness at different stages of loading. The stiffness in the multi-linear curve was used to calculate the vertical deflection with the inclusion of the effect of the shear deformation. The developed deflection curves were in close agreement to the curves obtained experimentally.

The panels with no shear connectors showed significant differences in their behavior due to the delamination of the boundary thickness of the AAC panels due to concrete shrinkage. The stiffness of these panels come solely from the friction between the concrete and AAC which was very sensitive to the degree of water absorption of AAC from concrete even with the roughening of the AAC surface. Such panels can not be relied on for construction.

Overall, AAC provided a viable alternative to foam as an inner core in reinforced concrete composite sandwich panels. AAC would further enhance the serviceability of the panels however with no notable increase in the ultimate capacity. A study of the shear connectors' stiffness is imperative to providing a better understanding of the behavior of the panels under flexure. With the availability of an accurate estimate of the shear connectors' stiffness, the behavior of the panels under flexure could be predicted with a good level of accuracy. Further research is needed to conduct a parametric study to look into different elements of design of these types of panels.

Appendix

According to [7], the shear force Q_1 associated with bending moment M_1 can be divided into two components.

$$-Q_1 = Dw_1''' = E_c(I - I_f)w_1''' + E_c(I_f)w_1''' \quad (8)$$

Where the first term on the right hand side of the equation represents the shear, neglecting the effect of the flexural rigidity of the faces, and the second term takes into account the effect of this flexural rigidity.

E_c is the modulus of elasticity of the faces which is made of concrete, I is the moment of inertia of the faces about the centroid of the sandwich and I_f is the sum of the moment of inertia of the faces about their own centroids,

$$I = bt^3/6 + btd^2/2$$

$$I_f = bt^3/6$$

The first term in Eq. 8 which represents a state of constant shear stress τ across the thickness of the core, assumed to be relatively weak, can be replaced by $-bd\tau$, thus Eq. 8 can be written in the form,

$$-Q_1 = -bd\tau + E_c(I_f)w_1''' \quad (9)$$

The shear stress τ will result in an additional deflection w_2

The relation between the core shear strain $\gamma$and the additional deflection is defined as, $\gamma = w_2'd/c$

τ can now be expressed in terms of w_2' as follows, $\tau = Gw_2'd/c$

where G is the shear modulus of core.

Hence Eq. 9 can now be expressed in the form,

$$-Q_1 = -AGw_2' + E_c(I_f)w_1''' \quad (10)$$

where $A = bd^2/c$

Rearranging terms and noting that $-Q_1 = Dw_1'''$, one can write, $w_2' = Q_1(1 - I_f/I)/AG$

The term $a^2 = AG/E_cI_f(1 - I_f/I)$is introduced.

$$E_cI_fw_2' = Q_1/a^2 \quad (11)$$

w_2 will be resisted by the stiff concrete faces resulting in additional shear force$Q_2 = -E_c(I_f)w_2'''$

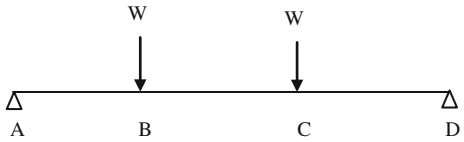

Fig. 15 Schematic for a panel under 4-Point load

The total shear force $Q = Q_1 + Q_2 = Q_1 - E_c(I_f)w_2'''$

The term w_2''' can be expressed in terms of Q_1 using Eq. 11

$$Q_1'' - a^2 Q_1 = -a^2 Q \tag{12}$$

The solution to the above differential equation is

$$-Q_1 = C_1 \cosh(ax) + C_2 \sinh(ax) + Q \tag{13}$$

where x is measured along the length of the panel, and C_1 and C_2 are constants.

Now, we will apply the general equation, Eq. 13, to the loading case under study.

Considering the slab loaded under a 4-pt loading where the load is applied at points B and C as shown in Fig. 15.

Since the load is symmetrical, only half the panel will be considered. The equations governing the deflection are as follows:

For Part A-B, with x measured arbitrary from point B,

$$\begin{aligned}
-Q_1 &= C_{1AB}\cosh(ax) + C_{2AB}\sinh(ax) - W\\
EIw_{1AB}''' &= C_{1AB}\cosh(ax) + C_{2AB}\sinh(ax) - W\\
EIw_{1AB}'' &= C_{1AB}\sinh(ax)/a + C_{2AB}\cosh(ax)/a\\
&\quad - Wx + 2C_{3AB}\\
EIw_{1AB}' &= C_{1AB}\cosh(ax)/a^2 + C_{2AB}\sinh(ax)/a^2\\
&\quad - Wx^2/2 + 2C_{3AB}x + C_{4AB}\\
EIw_{1AB} &= C_{1AB}\sinh(ax)/a^3 + C_{2AB}\cosh(ax)/a^3\\
&\quad - Wx^3/6 + C_{3AB}x^2 + C_{4AB}x + C_{5AB}\\
EI_f w_{2AB}' &= -C_{1AB}\cosh(ax)/a^2 - C_{2AB}\sinh(ax)/a^2\\
&\quad + W/a^2\\
EI_f w_{2AB} &= -C_{1AB}\sinh(ax)/a^3 - C_{2AB}\cosh(ax)/a^3\\
&\quad + Wx/a^2 - C_{6AB}\\
EI_f w_{2AB}'' &= -C_{1AB}\sinh(ax)/a - C_{2AB}\cosh(ax)/a\\
EI_f w_{2AB}''' &= -C_{1AB}\cosh(ax) - C_{2AB}\sinh(ax)
\end{aligned}$$

For Part B-C, with x measured arbitrary from mid-span

$$\begin{aligned}
-Q_1 &= C_{1BC}\cosh(ax) + C_{2BC}\sinh(ax)\\
EIw_{1BC}''' &= C_{1BC}\cosh(ax) + C_{2BC}\sinh(ax)\\
EIw_{1BC}'' &= C_{1BC}\sinh(ax)/a + C_{2BC}\cosh(ax)/a\\
&\quad + 2C_{3BC}\\
EIw_{1BC}' &= C_{1BC}\cosh(ax)/a^2 + C_{2BC}\sinh(ax)/a^2\\
&\quad + 2C_{3BC}x + C_{4BC}\\
EIw_{1BC} &= C_{1BC}\sinh(ax)/a^3 + C_{2BC}\cosh(ax)/a^3\\
&\quad + C_{3BC}x^2 + C_{4BC}x + C_{5BC}\\
EI_f w_{2BC}' &= -C_{1BC}\cosh(ax)/a^2 - C_{2BC}\sinh(ax)/a^2\\
EI_f w_{2BC} &= -C_{1BC}\sinh(ax)/a^3 - C_{2BC}\cosh(ax)/a^3\\
&\quad - C_{6BC}\\
EI_f w_{2BC}'' &= -C_{1BC}\sinh(ax)/a - C_{2BC}\cosh(ax)/a\\
EI_f w_{2BC}''' &= -C_{1BC}\cosh(ax) - C_{2BC}\sinh(ax)
\end{aligned}$$

To determine the constants of integration, the boundary conditions and requirements for continuity at B will be considered.

Four boundary conditions are available in AB, with x measured arbitrary from point B are,

(1) $w_{1AB} = 0$ at $x = 0$ (Arbitrary)

$C_{2AB} = -C_{1AB}\tanh(aL)$

(2) $w_{2AB} = 0$ at $x = 0$ (Arbitrary)

$C_{3AB} = WL/2$

(3) $M = -WL$ at $x = 0$

$C_{2AB}/a^3 = -C_{6AB}$

(4) $w_{1AB}'' = 0$ at $x = L$

$C_{2AB}/a^3 = -C_{5AB}$

In part BC with x measured from midspan, five boundary conditions are available as follows,

(5) $w_{1BC} = 0$ at $x = 0$ (Arbitrary)

$C_{3BC} = WL/2$

(6) $w_{2BC} = 0$ at $x = 0$ (Arbitrary)

$C_{4BC} = 0$

(7) $w_{2BC}' = 0$ at $x = 0$ (Arbitrary)

$C_{1BC} = 0$

(8) $w_{1BC}' = 0$ at $x = 0$ (Arbitrary)

$$C_{2BC}/a^3 = -C_{5BC}$$

(9) $M = -WL$ at $x = 0$

$$C_{2BC}/a^3 = -C_{6BC}$$

Using continuity conditions at point B,

(10) w_1' is continuous

$$C_{1AB}/a^2 + C_{4AB} = C_{2BC}\sinh(aL/2)/a^2 + WL^2/2$$

(11) w_2' is continuous

$$C_{4AB} = -W/a^2 + WL^2/2$$

(12) w_1'' is continuous

$$C_{2BC}\cosh(3aL/2) = -W\sinh(aL)$$

The summation of w for part AB can be written as

$$w_{AB} = \left[\left(-C_{1AB}\sinh(ax)/a^3 - C_{2AB}\cosh(ax)/a^3 - C_{6AB} + Wx/a^2\right)/EI_f\right][1 - (I_f/I)] + \left[\left(WL^2x/2 + WLx^2/2 - Wx^3/6\right)/EI\right] \quad (14)$$

The maximum deflection for this part occurs at point x (one third of the panel length) = 93 cm

The summation of w for part BC can be written as

$$w_{BC} = \left[\left(C_{2BC}(1 - \cosh(ax))/a^3\right)/EI_f\right][1 - (I_f/I)] + \left[\left(WLx^2/2\right)/EI\right] \quad (15)$$

The maximum deflection for this part occurs at x (located at midspan) = 46.5 cm

The maximum deflection at midspan is the summation of the maxima for Eqs. 14 and 15.

References

1. Seeber K et al (1997) State-of-the-art report on precast/prestressed sandwich wall panels: PCI Committee report. PCI J 42(2):1–61
2. Pfeifer DW, Hanson JA (1964) Precast Concrete Wall Panels: Flexural Stiffness of Sandwich Panels. Special Publication SP-11, American Concrete Institute, Farmington Hills, MI, pp 67–86
3. Bush TD Jr, Stine GL (1994) Flexural behavior of composite precast sandwich panels with continuous truss connectors. PCI J 39(2):112–121
4. Pessiki S, Mlynarczyk A (2003) Experimental evaluation of the composite behavior of precast concrete sandwich wall panels. PCI J 48(2):54–71
5. Salmon DC, Einea A, Tadros MK, Culp TD (1997) Full scale testing of precast concrete sandwich panels. ACI Struct J 94(4):354–362
6. Naito C, Hoemann J, Bewick B, Hammons M (2009) Evaluation of shear tie connectors for use in insulated concrete sandwich panels. Air Force Research Laboratory Report, AFRL-RX-TY-TR-2009-4600
7. Allen HG (1969) Analysis and design of structural sandwich panels. Pergamon Press, Oxford
8. Frostig Y, Baruch M, Vilnay O, Sheinman I (1991) Bending of nonsymmetric sandwich beams with flexible core-bending behavior. J Eng Mech 117(9):1931–1952
9. Thomsen OT (1992) Analysis of local bending effects in sandwich panels subjected to concentrated loads. In: Proceeding of Second International Conference on Sandwich Construction. March 9–12, University of Florida, Gainesville, USA
10. Frostig Y, Baruch M, Vilnay O, Sheinman I (1992) Higher-order theory for sandwich beam behavior with transversely flexible core. J Eng Mech 118(5):1026–1043
11. Straalen IJV. (2000) Comprehensive overview of theories for sandwich panels. In: Proceedings of Workshop on Modeling of Sandwich Structures and Adhesive Bonded Joints, Porto
12. Salmon DC, Einea A (1995) Partially composite sandwich panel deflections. J Struct Eng 121(4):778–783